



## Adsorption Performance of Acidic Modified Fly Ash: Box–Behnken Design

İlhan Küçük<sup>1\*</sup>, Pınar Üstündağ<sup>2</sup>

<sup>1</sup>Department of Chemistry, Faculty of Arts and Sciences, Muş Alparslan University, Muş, Türkiye.

<sup>2</sup>Health Sciences, Muş Alparslan University, Muş, Türkiye.

**Abstract:** Fly ash (FA) and modified fly ash (mFA) were used as adsorbents to remove methylene blue (MB) dye from aqueous solutions. The adsorbents were characterized using crystal structures with XRD, surface functional groups with FTIR, and surface morphologies with SEM. Response surface methodology (RSM) with Box-Behnken design (BBD) was used to optimize adsorption parameters such as MB dye concentration (A: 10-20 mg/L), solution pH (B: 3-11), and contact time (C: 30-180 min). ANOVA analysis shows the significant interactions between initial concentration, solution pH value, and solution pH value, contact time was found to be significant in the removal of MB ( $p$ -value= $\leq 0.0001, 0.0040$ ), whereas between the effect of initial concentration and contact time was not significant ( $p$ -value = 0.0881). The adsorption kinetics followed the pseudo-second-order (PSO) kinetic model and the adsorption isotherm followed the Langmuir model. At 28°C, the adsorption capacity of fly ash-HNO<sub>3</sub> for MB was found to be 7.67 mg/g.

**Keywords:** Fly Ash, ANOVA, Adsorption, Box–Behnken design, Methylene blue.

**Submitted:** September 26, 2023. **Accepted:** February 19, 2024.

**Cite this:** Küçük İ, Üstündağ P. Adsorption Performance of Acidic Modified Fly Ash: Box–Behnken Design. JOTCSA. 2024;11(2):699-708.

**DOI:** <https://doi.org/10.18596/jotcsa.1366346>

**\*Corresponding author's E-mail:** [i.kucuk@alparslan.edu.tr](mailto:i.kucuk@alparslan.edu.tr)

### 1. INTRODUCTION

Fly ash (FA) is a product made from coal-burning power plants. Every year, EU countries produce around two million tons of fly ash, but only a small portion of it is utilized (1). FA has numerous applications, including its use in cementitious products, construction sites such as highway road bases, and as an effective sorbent for eliminating heavy metals, organics, and dyes from water (2). Although FA has many positive uses, its production rate exceeds its consumption rate. So, FA disposal poses a significant problem due to its detrimental impact on air, water, and soil (3).

FA can be used as an inexpensive adsorbent to eliminate dyes, heavy metals, and organics from wastewater (4). This is due to its low cost, availability, and environmentally friendly features (5). However, the low surface area and crystalline structure of FA waste result in a low adsorption capacity. To improve the adsorption efficiency of dye-contaminated wastewater, the modification of FA with chemical and physical methods has been studied. Many researchers have experimented with various methods to modify FA to adsorb different

dyes. Treatment with different methods has been found to increase the adsorption capacity (6).

Every day, clean water supplies are at risk of being contaminated by harmful substances like synthetic dyes, heavy metals, medicines, pesticides, and other pollutants. Synthetic dyes, in particular, can be extremely dangerous even in small amounts, as they can cause cancer and mutations (7). These dyes are commonly used in various industries such as textiles, paper, pulp, tanneries, and pharmaceuticals due to their affordability, vibrant hues, ability to withstand environmental factors, and ease of application (8). The widespread use of these dyes has led to a significant amount of pollution being released into water systems. This pollution has harmful impacts on the environment and poses a threat to human health (9). Efficient treatment of dye effluent is necessary before it can be released into a water body. Several methods have been devised for removing dyes from industrial wastewater, such as electrocoagulation (10), coagulation (11), photocatalysis (12), cation-exchange membrane (13), and adsorption (14). Out of all the different treatment methods available, adsorption is considered to be the most favorable

due to its easy implementation, high removal efficiency, and minimal secondary pollution (15).

The research aims to enhance the adsorption capacity of FA, which is produced in large quantities in our country and around the world, for methylene blue through acidic modification. The study involved characterizing the modified FAs and conducting tests using the modification that demonstrated the highest adsorption capacity, as well as kinetic and isotherm equations. Additionally, the Box-Behnken design (BBD) was utilized to optimize the adsorption of MB dye statistically and maximize its efficiency.

## 2. METHODS AND MATERIALS

### 2.1. Materials and Reagents

The FA was obtained from a thermal power plant (Afşin, Elbistan, Türkiye). Hydrochloric acid (HCl, 0.5 M, J.T. Baker, Poland), sulfuric acid (H<sub>2</sub>SO<sub>4</sub>, ~96-99%, Merck Germany), and nitric acid (HNO<sub>3</sub>, ~65%, Merck, Germany) were procured. Methylene blue

(Isolab, Türkiye, λ<sub>max</sub>, 663 nm) was used in the adsorption process as adsorbates.

### 2.2. Preparation of the FA

The fly ash obtained from Afşin/Elbistan was washed with distilled water and dried at 105 °C in the oven until constant weight was reached. The dried fly ash earned a stable weight and was thoroughly ground using an agate mortar. Three different conical flask samples, each weighing 25 grams, were added to the obtained fly ash, and 0.1 M H<sub>2</sub>SO<sub>4</sub>, HCl, and HNO<sub>3</sub> were added to each sample. Partial carbon dioxide release was observed. The mixture was stirred at 400 rpm at room temperature for 6 hours. The mixture was then filtered through filter paper (coarse filter paper), and the resulting modified fly ash was washed with distilled water until it reached a pH of 7.

The Box-Behnken method was studied with the help of the Design Expert -13 program and working conditions are given in Table 1.

**Table 1.** Adsorption conditions.

Run	A: Initial Concentration	B: pH	C: Contact time	Response: Adsorption amount
1	10	3	105	5.1
2	10	7	30	5
3	20	7	180	9.7
4	15	11	180	10.3
5	15	7	105	7
6	15	7	105	7.2
7	15	3	180	5.5
8	20	11	105	12
9	10	7	180	6.7
10	15	7	105	6.7
11	15	7	105	7.1
12	15	3	30	4.5
13	15	11	30	7.6
14	10	11	105	7.3
15	20	3	105	5.4
16	20	7	30	7.2
17	15	7	105	7.1

### 2.3. Adsorption Procedure

For the adsorption study, 0.5 g of methylene blue (C<sub>16</sub>H<sub>18</sub>ClN<sub>3</sub>S, λ<sub>max</sub> = 663 nm) was taken and dissolved in 1000 mL of distilled water to prepare the stock solution. This stock solution was used in all adsorption processes. Isotherm studies were conducted at three different temperatures (301, 310, and 321 K) with initial concentrations ranging from 5 to 25 ppm for a duration of 3 h. Additionally, kinetic studies were carried out for initial concentrations ranging from 10 to 20 ppm for a duration of 3 h. Equation 1 was used to determine the results.

$$qe = \frac{(Co - Ce)V}{W} \quad (1)$$

pH adjustments were made with 0.01, 0.1 M HCl, and 0.01 and 0.1 M NaOH solutions.

### 2.4. Fly Ash Analysis

The surface morphologies of fly ash were determined using SEM (scanning electron microscope model LEO-EVO 40). FTIR analysis was analyzed in an Agilent Cary 630 Infrared Spectrophotometer

equipped with a spectrum range of 400-4000 cm<sup>-1</sup>, resolution 2 cm<sup>-1</sup>, to observe different functional groups. XRD spectrum of the fly ash was analyzed in a PANalytical Empyrean equipped with a spectrum range of 10-80 2θ, X-ray generator 4 kW to observe crystallization. UV-Vis Analysis was performed with an Agilent Cary 60 device.

## 3. RESULTS AND DISCUSSION

### 3.1. Characterization of FAs

FT-IR analysis is a widely used method to investigate structural modifications in substances (16). This particular study analyzed the infrared spectra of FA and mFA. The spectra were evaluated in four distinct regions that correspond to vibrations of Si-Al, C, S, and OH bonds. The number of vibrations in each wavelength was assessed to identify any differences between them. The results from FTIR analysis helped to determine the surface structures of molecules, which are depicted in Figure 1 A. The Si-O bonds associated with Al-O vibrations occur at frequencies

of 593 and 604  $\text{cm}^{-1}$ . Additionally,  $\text{CO}_3^{2-}$  can be seen at 1426  $\text{cm}^{-1}$  (17).

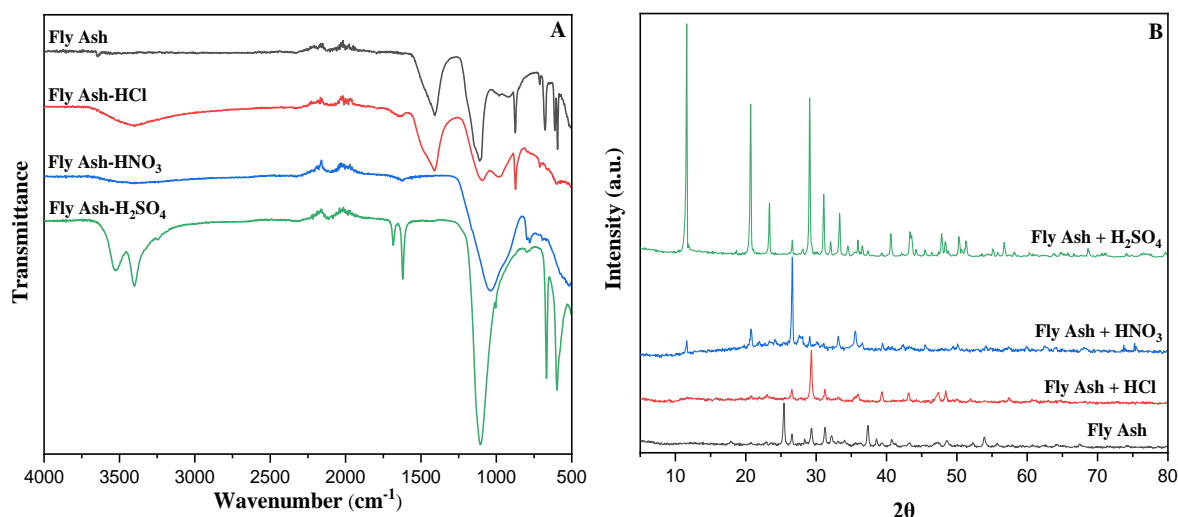


**Figure 1: A.** FT-IR spectrum **B.** X-ray diffraction spectrum.

Meanwhile, the vibrations of Si-O bonds in cage assemblies are observed at a frequency of 908  $\text{cm}^{-1}$ , and vibrations of Si-O-Si bonds are observed at a frequency of 1040  $\text{cm}^{-1}$  (18). The band at about 1430  $\text{cm}^{-1}$  is from sodium carbonate inclusion due to the reaction of residual sodium with atmospheric  $\text{CO}_2$  (16). Additionally, the weak peaks at 1660 may be due to unburned carbons in fly ash, caused by C=O

and C=C stretching and bending (16). The broad band at 3490–3390  $\text{cm}^{-1}$  corresponded to stretching vibrations of (Al)O-H and (Si)O-H bonds (19). The peaks in the untreated sample were slightly increased after modification which illustrates the attachment of the carboxylic group to the surface of fly ash. This is an indication that carboxylic groups are attached to the surface of fly ash.

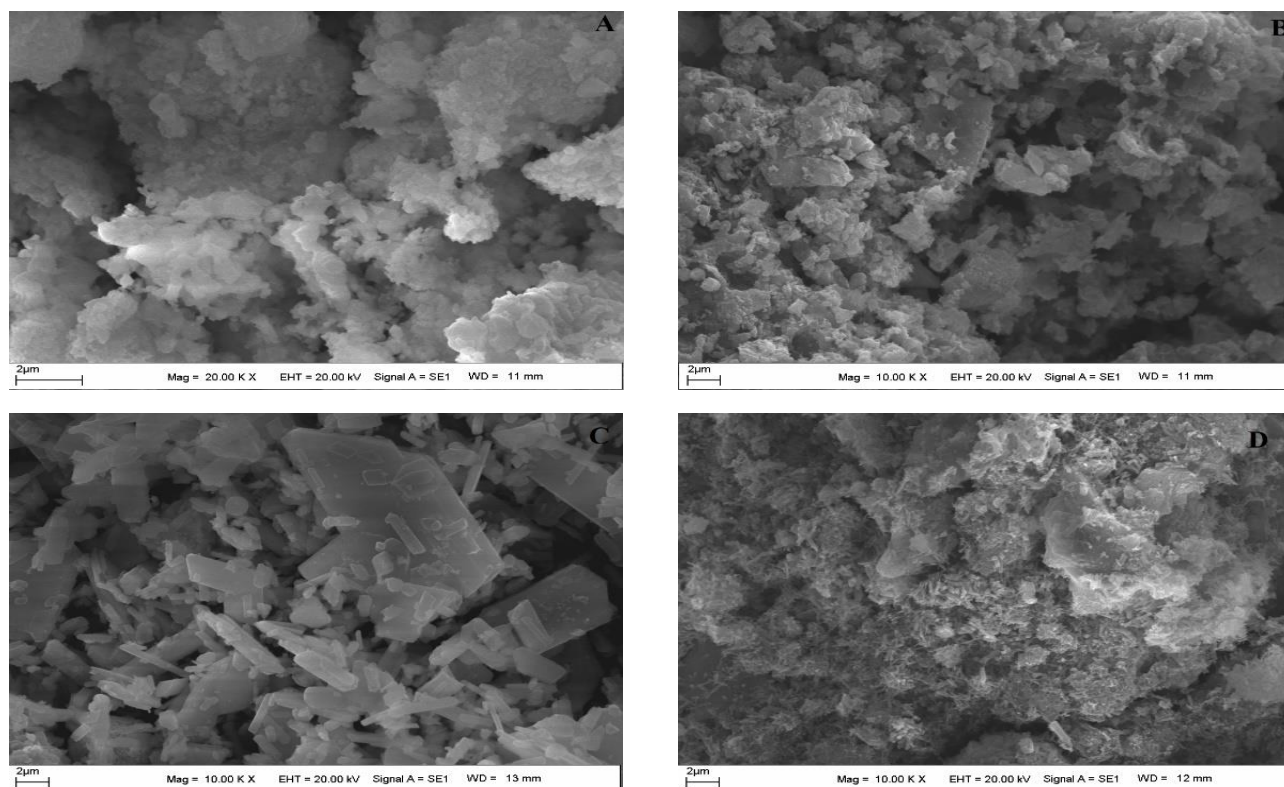


**Figure 2: A.** Fly Ash **B.** Fly Ash + HNO<sub>3</sub> **C.** Fly Ash + H<sub>2</sub>SO<sub>4</sub> **D.** Fly Ash + HCl.

The X-ray diffraction pattern presented in Figure 1 B determined crystallographic information about the FAs. The peaks within the 2θ angle range of 5 to 80 were identified based on peak position data. The diffractogram of FAs exhibits various peaks related to the primary chemical components, namely oxides.

These components include quartz, corundum, mullite, and hematite, along with other complex crystalline phases such as anorthite, goethite, albite, portlandite, gibbsite, and magnesium hydroxide (20). Most of the peaks in the fly ash diffractogram and modified fly ash were between 20-45.

Furthermore, the quartz and corundum peaks with the highest intensities were located between 20 and 30. The characteristic peaks of quartz and corundum are: 21°, 27°, 37° and 26°, 35°, 39° respectively. Mullite and hematite structures exhibit peaks at approximately 25-40° and 34-38°, respectively. Based on the results obtained, it is evident that the structure contains a high concentration of oxides.

SEM images reveal material morphology and surface texture. Figure 2 shows micrographs of fly ash and modified fly ash. Modifying fly ash brings about alterations in its surface appearance. The HNO<sub>3</sub> modification causes the structure to adopt a more particulate form, whereas the H<sub>2</sub>SO<sub>4</sub> modification leads to the emergence of more pronounced and abundant crystal formations within the structure. Additionally, crystal structures are partially formed through the HCl modification.

### 3.2. Box–Behnken design

MB adsorption tests were designed using Design Expert 13.0 software, and a quadratic polynomial regression model was utilized to predict the response (Equation 2).

$$Y = \beta_0 + \sum \beta_i X_i + \sum \beta_{ii} X_i^2 + \sum \sum \beta_{ij} X_i X_j \quad (2)$$

Y shows the response factor;  $\beta_0$  is the constant;  $X_i$  and  $X_j$  are coded as the factors;  $\beta_i$ ,  $\beta_{ii}$ , and  $\beta_{ij}$  are coefficients of studied factors. BBD provided 17 experiments for optimizing factors affecting MB dye removal including A: Initial concentration (10–20 mg/g), B: pH (3–11), and C: Contact time (30–180 min). Table 1 presents data obtained from BBD regarding the removal of MB dye.

**Table 2:** ANOVA analysis.

Source	Sum of Squares	df	Mean Square	F-value	p-value
<b>Model</b>	61.96	9	6.88	168.78	< 0.0001
A-Initial Concentration	13.01	1	13.01	318.86	< 0.0001
B-pH	34.86	1	34.86	854.74	< 0.0001
C-Contact Time	7.80	1	7.80	191.27	< 0.0001
AB	4.84	1	4.84	118.67	< 0.0001
AC	0.1600	1	0.1600	3.92	0.0881
BC	0.7225	1	0.7225	17.71	0.0040
A <sup>2</sup>	0.3853	1	0.3853	9.45	0.0180
B <sup>2</sup>	0.0684	1	0.0684	1.68	0.2362
C <sup>2</sup>	0.1253	1	0.1253	3.07	0.1231
<b>Residual</b>	0.2855	7	0.0408		
Lack of Fit	0.1375	3	0.0458	1.24	0.4059
Pure Error	0.1480	4	0.0370		
<b>Cor Total</b>	62.24	16			

BBD was used to design 17 experiments (as shown in Table 1) for testing three independent parameters that may significantly affect MB removal. BBD in RSM was used to investigate the effects of three independent variables on MB removal: Initial concentration (A), pH (B), and Contact time (C). The ANOVA analysis of experimental data for MB removal is presented in Table 2. ANOVA results were analyzed using p-values, sum of squares, and F-values to determine significant factors. The model's statistically significant F-value of 168.78 for MB removal has a corresponding p-value < 0.0001 (21). The adjusted R<sup>2</sup> of 0.989 and R<sup>2</sup> value of 0.995 indicate a strong correlation between predicted and actual values. According to Table 2, model term values with Prob > F < 0.0500 indicate that factors are significant under the chosen conditions. The significant model terms are linear terms of A, B, and C, quadratic terms of A<sup>2</sup>, B<sup>2</sup>, and C<sup>2</sup>, and interaction

between AB, AC, and BC. To enhance the model fit, insignificant terms with p-value > 0.05 were excluded. Equation (4) expresses the polynomial relationship between examined parameters and MB removal.

$$\text{MB removal (mg/g)} = 8,59 - 0,55 A - 0,56 B + 0,002 C + 0,055 AB + 0,0005 AC + 0,001 BC + 0,012A^2 + 0,008 B^2 - 3,06 \times 10^{-5} C^2$$

The interactions between initial concentration (A), solution pH value (B), and solution pH value (B), contact time (C) were found to be significant on the removal of MB (p-value=< 0.0001, 0.0040), whereas between the effect of initial concentration (A) and contact time (C) was not significant (p-value = 0.0881). The three-dimensional (3D) surface for interaction between initial concentration (A), solution pH (B), and contact time (C) was given in Figure 3.

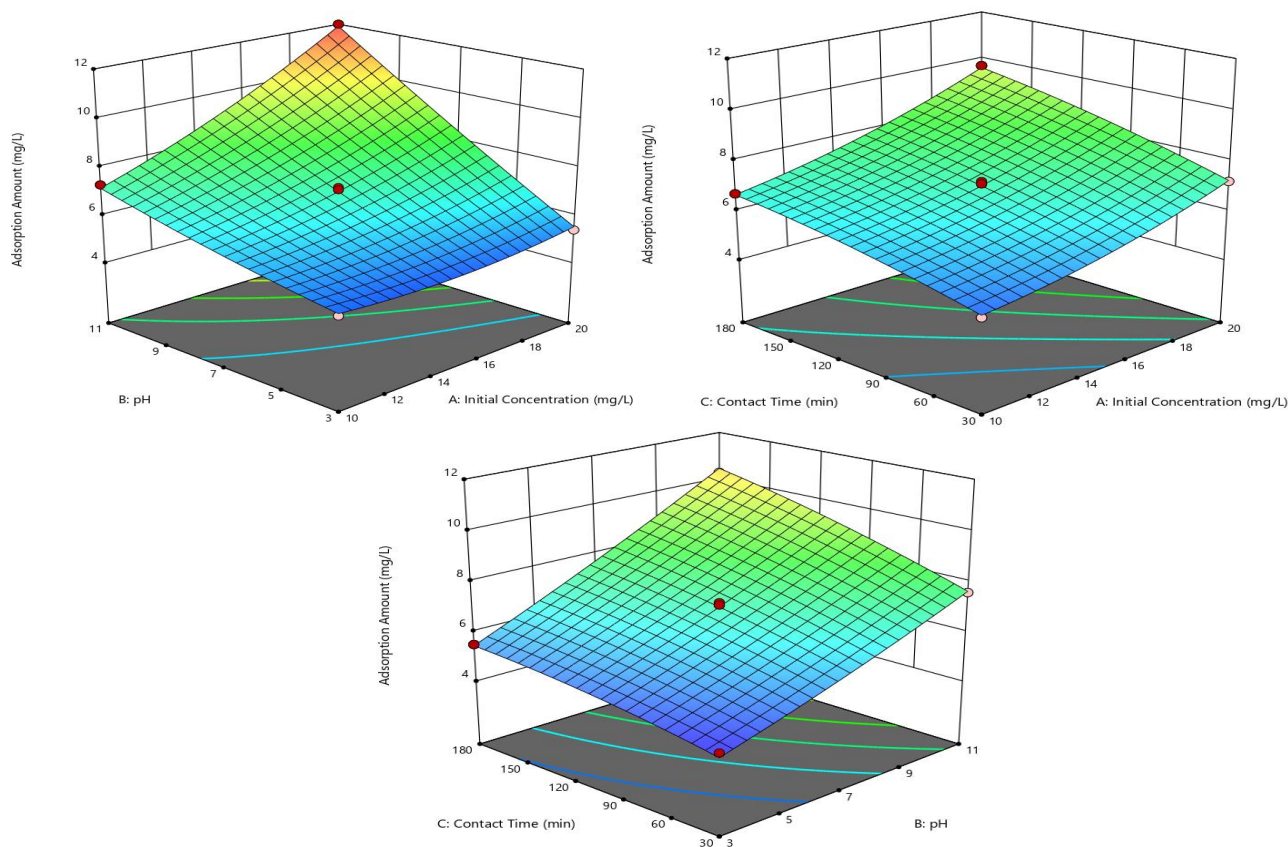


**Figure 3:** 3D response surface plot of MB removal.

The graph in Figure 4 illustrates how MB adsorption changes with varying initial concentrations, pH, and contact times. The concentration of the pollutant significantly affects the adsorption capacity of the adsorbent. The initial concentration of the MB was varied from 10 mg/L to 20 mg/L, resulting in an increase in uptake from 6.6 mg/g to 7.7 mg/g onto FA-HNO<sub>3</sub>. Enhancement in adsorption capacity can be explained by the higher concentration of MB, which offers more molecules to be diffused into internal pores of FA-HNO<sub>3</sub> and reach active adsorption sites (22). The pH of an adsorption system significantly affects the adsorbent's surface characteristics, as well as the adsorbate's ionization and speciation. The effect of pH on the uptake of MB was studied across a pH range of 3 to 11. A significant increase in adsorption capacity occurs from pH 3 to 11, with a nearly two-fold increase in capacity. At low pH, the electron-rich active site on the sorbent surface was easily protonated, so less

available for MB cations adsorption. So, at low pH levels, its ability to adsorb is significantly reduced, causing a decrease in its adsorption capacity (23). The adsorption capacity of the adsorbent is significantly impacted by the duration of the pollutant's contact with the system. The adsorption of MB was initially very fast, with approximately 60% of the dye being adsorbed within the first 30 min. As the contact time between adsorbate and adsorbent increased, the uptake of MB dye gradually increased up to 180 min. The fast initial adsorption rate may be attributed to a higher number of available active sites, in terms of functional groups and pores, on the surface of the adsorbent during the initial stage of the adsorption process. However, as the adsorption process continues, the build-up of dye molecules on the surface of the adsorbent hinders the diffusion of molecules into pores, which leads to a slower adsorption rate (24).

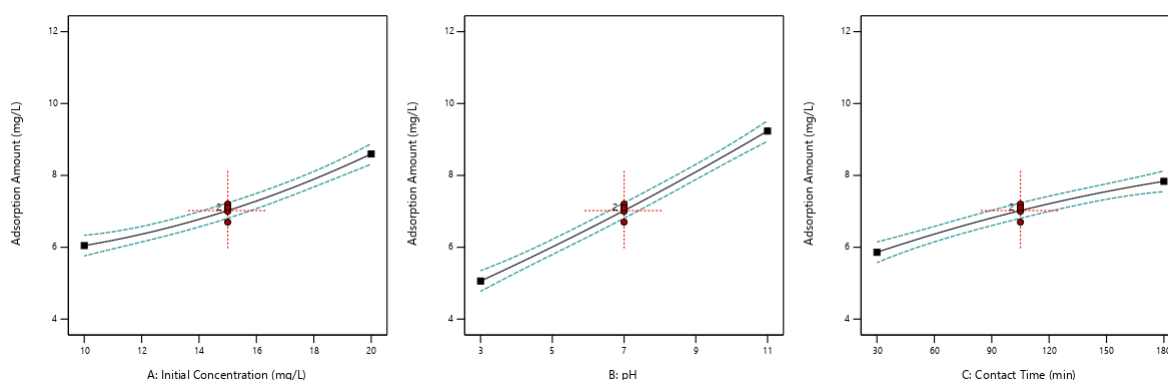


**Figure 4:** BBD of the effect of initial concentration, pH, and contact time.

### 3.3. Adsorption Studies

#### 3.3.1 Adsorption isotherms

Understanding the interaction between Fly ash-  $\text{HNO}_3$  and MB dye requires analyzing the adsorption isotherm. To determine the ability of Fly ash- $\text{HNO}_3$  to adsorb MB dye, the experimental data was fitted using linear forms of Langmuir, Freundlich, Temkin, and D-R models (25). These models are expressed by Eqs. (3)–(6) and help determine the adsorption capacity of Fly ash- $\text{HNO}_3$ .

$$\frac{C_e}{q_e} = \frac{1}{K_L q_m} + \frac{C_e}{q_m} \quad (3)$$

$$\log q_e = \log K_F + \frac{1}{n} \log C_e \quad (4)$$

$$q_e = \frac{RT}{B_T} \ln K_T + \frac{RT}{B_T} \ln C_e \quad (5)$$

$$\ln q_e = \ln q_s - k_{ad} \varepsilon^2 \quad (6)$$

$K_L$  (L/mg) is Langmuir isotherm constant,  $q_m$  (mg/g) is maximum adsorption capacity,  $K_F$  (mg/g) is Freundlich constant,  $T$  (K) is temperature in Kelvin,  $n$  is adsorption intensity,  $K_T$  (L/mg) is Temkin constant;  $b_T$  (J/mol) is heat of adsorption;  $R$  (8.314 J/mol·K) is universal gas constant;  $\varepsilon$ , is polanyi constant.

In Figure 5, the plot and function of isotherms are illustrated, while their detailed information is presented in Table 3. According to Table 3, it was observed that Langmuir isotherm was the most appropriate model for describing the homogeneous surface and monolayer adsorption of MB onto the adsorbent surface, with the highest  $R^2$  value of 0.99. At a temperature of 28 °C, the maximum adsorption capacity ( $q_m$ ) of the adsorbent for MB was determined to be 7.67 mg/g.

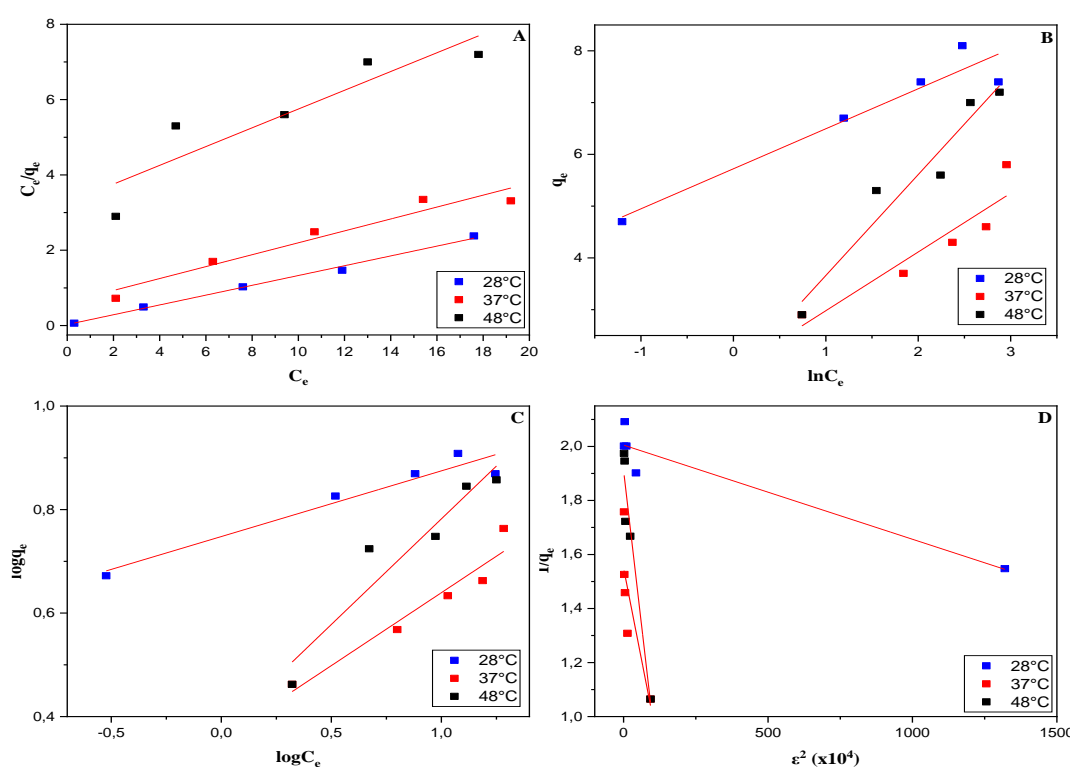


Figure 5: A. Langmuir B. Temkin C. Freundlich D. D-R.

Table 3. Isotherm constant.

°C	Langmuir			Freundlich			
	$q_m$	$K_L$	$R^2$	$K_F$	$n$	$R^2$	
28	7.67	4.96	0.997	5.59	7.88	0.966	
37	6.32	0.25	0.969	2.27	3.55	0.965	
48	4.01	0.07	0.911	2.36	2.45	0.953	
°C	D-R			Temkin			
	$q_s$	$K_{ad}$	$E$	$R^2$	$B_T$	$K_T$	$R^2$
28	7.42	$3.4 \times 10^{-4}$	37.87	0.956	3237	1637	0.960
37	4.70	$5.4 \times 10^{-3}$	9.57	0.835	2270	5.07	0.928
48	6.75	$9.2 \times 10^{-3}$	7.41	0.972	1368	2.40	0.969

#### 3.3.2 Adsorption kinetics

The kinetics of adsorption can provide valuable insights into the mechanism of MB adsorption. To determine the mechanism of adsorption of MB onto fly ash and modified fly ash, we applied kinetic models such as the pseudo-first-order (PFO),

Elovich, and pseudo-second-order (PSO) models. We examined experimental results of varying initial MB concentrations. The linear equations for PFO, Elovich, and PSO, models are explained in equations 7, 8, and 9, respectively (26).

$$\ln(q_e - q_t) = \ln q_e - k_1 t \quad (7)$$

$$q_e = \frac{1}{b} \ln(ab) + \frac{1}{b} \ln(t) \quad (8)$$

$$\frac{t}{q_t} = \frac{1}{k_2 q_e^2} + \frac{t}{q_e} \quad (9)$$

$q_e$  (mg/g) is the amount of MB adsorbed by fly ash at equilibrium,  $q_t$  (mg/g) is the amount of MB adsorbed by fly ash at the time (t);  $k_1$  (1/min) and  $k_2$  (g/mg min) are rate constants of PFO and PSO respectively; a, b is Elovich constant.

In Figure 6, the plot and function of isotherms are illustrated, while their detailed information is presented in Table 4. In Table 4, the  $R^2$  correlation coefficients from the pseudo-second-order model were found to be over 0.995, higher than those of

the pseudo-first-order model. This indicates that the pseudo-second-order model best describes the kinetics of MB adsorbed onto FA. Additionally, the calculated  $q_e$ , cal values from the pseudo-second-order model closely match the experimental  $q_e$ , exp values, whereas the  $q_e$ , cal values from the pseudo-first-order model are lower than the  $q_e$ , exp values. These results further support that the adsorption of MB onto FA from aqueous solution follows the pseudo-second-order model well. Similar phenomena have been observed in MB adsorption on other natural products. The pseudo-second-order model assumes that the rate-determining step involves chemical adsorption with valence forces through the sharing or exchange of electrons between the adsorbent and the adsorbate.

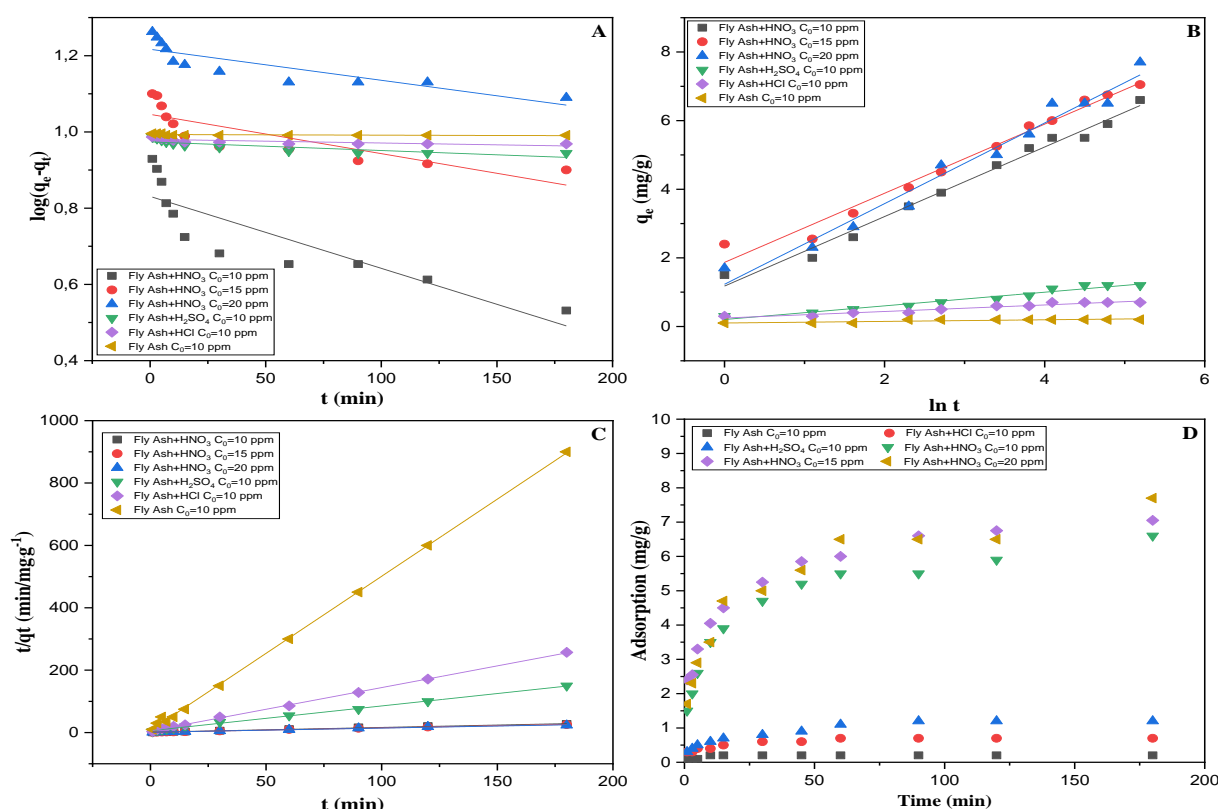


Figure 6: A. PFO B. Elovich C. PSO D. Effect of initial concentration and contact time.

Table 4. Kinetic Constant.

Adsorbent	$C_0$	Pseudo-First Order			Pseudo-Second Order		
		$k_1$	$q_e$	$R^2$	$k_2$	$q_e$	$R^2$
Fly ash-HNO <sub>3</sub>	10	$1.8 \times 10^{-3}$	2.29	0.871	0.019	6.57	0.996
Fly ash-HNO <sub>3</sub>	15	$1.0 \times 10^{-3}$	2.84	0.847	0.023	7.14	0.999
Fly ash-HNO <sub>3</sub>	20	$8.1 \times 10^{-4}$	3.37	0.857	0.015	7.57	0.995
Fly ash-H <sub>2</sub> SO <sub>4</sub>	10	$2.2 \times 10^{-4}$	2.64	0.842	0.109	1.25	0.999
Fly ash-HCl	10	$9.6 \times 10^{-5}$	2.66	0.764	0.385	0.71	0.999
Fly ash	10	$1.6 \times 10^{-5}$	2.69	0.481	3.715	0.20	0.999
Elovich							
Adsorbent	$C_0$	a	b	$R^2$			
Fly ash-HNO <sub>3</sub>	10	3.26	0.98	0.993			
Fly ash-HNO <sub>3</sub>	15	6.44	0.99	0.989			
Fly ash-HNO <sub>3</sub>	20	3.35	0.85	0.985			
Fly ash-H <sub>2</sub> SO <sub>4</sub>	10	1.02	5.03	0.979			
Fly ash-HCl	10	1.26	10.49	0.967			
Fly ash	10	1.74	42.55	0.832			

Table 5 presents a comparison of the maximum adsorption capacity, referred to as  $q_m$ , for the adsorption of dyes onto different types of fly ash (FA). In this study, the  $q_x$  values obtained for the adsorption of dyes were found to be comparable to those reported in previous research. However, it is noteworthy that the  $q_m$  values observed for the dyes in this study were relatively lower when compared to

findings from other investigations. Despite the relatively lower adsorption capacity exhibited by the fly ash examined in this study, its potential as an adsorbent for dye removal remains of interest. This is primarily due to its advantageous characteristics such as being cost-effective and readily available as a waste material.

**Table 5.** Comparison of dye adsorption on fly ash.

Dye	Fly ash type	$q_m$ (mg/g)	References
Acid red 1	Coal FA	92.59	(27)
Acid red 1	Coal FA-NaOH	12.66	(27)
Acid red 91	FA	1.46	(28)
Acid Blue 9	FA	4.31	(28)
Acid Blue193	FA	22.08	(29)
Acid Black 1	FA	18.94	(29)
Reactive Red 23	FA	5.04	(29)
Reactive Black 5	FA	7.94	(30)
Reactive Red 198	Coal FA	47.26	(31)
Reactive Yellow 84	Coal FA	37.26	(31)
Methylene Blue	FA	7.67	This study

#### 4. CONCLUSION

Fly ash and modified fly ash were applied for the removal of MB. Response surface methodology (RSM) was used to optimize key adsorption parameters, and an analysis of variance (ANOVA) was performed. The interactions between initial concentration (A), solution pH value (B), and solution pH value (B), contact time (C) were found to be significant in the removal of MB (p-value= $< 0.0001$ , 0.0040), whereas the effect of initial concentration (A) on contact time (C) was not significant (p-value = 0.0881). Equilibrium data obtained at various temperatures fit well with the Langmuir isotherm model, as compared to the Freundlich and Temkin isotherm models. The maximum monolayer adsorption capacities were found to be 7.67, 6.32, and 4.01 mg/g at 28, 37, and 48 °C, respectively, and were spontaneous at all studied temperatures. This material has the potential for wider applications, including the removal of heavy metals, pesticides, and other colorless organic pollutants in water.

#### 5. ACKNOWLEDGEMENTS

This project is funded by TUBITAK 2209-A program.

#### 6. REFERENCES

- Buema G, Harja M, Lupu N, Chiriac H, Forminte L, Ciobanu G, et al. Adsorption Performance of Modified Fly Ash for Copper Ion Removal from Aqueous Solution. Water [Internet]. 2021 Jan 16;13(2):207. Available from: [<URL>](#).
- Gao M, Ma Q, Lin Q, Chang J, Ma H. A novel approach to extract SiO<sub>2</sub> from fly ash and its considerable adsorption properties. Mater Des [Internet]. 2017 Feb;116:666–75. Available from: [<URL>](#).

- Ohenoja K, Pesonen J, Yliniemi J, Illikainen M. Utilization of Fly Ashes from Fluidized Bed Combustion: A Review. Sustainability [Internet]. 2020 Apr 8;12(7):2988. Available from: [<URL>](#).
- Zhang M, Mao Y, Wang W, Yang S, Song Z, Zhao X. Coal fly ash/CoFe<sub>2</sub>O<sub>4</sub> composites: a magnetic adsorbent for the removal of malachite green from aqueous solution. RSC Adv [Internet]. 2016;6(96):93564–74. Available from: [<URL>](#).
- Taufiq A, Hidayat P, Hidayat A. Modified coal fly ash as low cost adsorbent for removal reactive dyes from batik industry. Ma'mun S, Tamura H, Purnomo MRA, editors. MATEC Web Conf [Internet]. 2018 Feb 28;154:01037. Available from: [<URL>](#).
- Hussain Z, Chang N, Sun J, Xiang S, Ayaz T, Zhang H, et al. Modification of coal fly ash and its use as low-cost adsorbent for the removal of directive, acid and reactive dyes. J Hazard Mater [Internet]. 2022 Jan;422:126778. Available from: [<URL>](#).
- Acisli O, Acar I, Khataee A. Preparation of a fly ash-based geopolymer for removal of a cationic dye: Isothermal, kinetic and thermodynamic studies. J Ind Eng Chem [Internet]. 2020 Mar;83:53–63. Available from: [<URL>](#).
- Chandarana H, Subburaj S, Kumar PS, Kumar MA. Evaluation of phase transfer kinetics and thermodynamic equilibria of Reactive Orange 16 sorption onto chemically improved Arachis hypogaea pod powder. Chemosphere [Internet]. 2021 Aug;276:130136. Available from: [<URL>](#).
- Malek NNA, Jawad AH, Ismail K, Razuan R, ALothman ZA. Fly ash modified magnetic chitosan-polyvinyl alcohol blend for reactive orange 16 dye removal: Adsorption parametric optimization. Int J Biol Macromol [Internet]. 2021 Oct;189:464–76. Available from: [<URL>](#).
- Hendaoui K, Trabelsi-Ayadi M, Ayari F. Optimization and mechanisms analysis of indigo dye removal using

- continuous electrocoagulation. Chinese J Chem Eng [Internet]. 2021 Jan;29:242-52. Available from: [<URL>](#).
11. Demissie H, An G, Jiao R, Ritigala T, Lu S, Wang D. Modification of high content nanocluster-based coagulation for rapid removal of dye from water and the mechanism. Sep Purif Technol [Internet]. 2021 Mar;259:117845. Available from: [<URL>](#).
12. Ahmad Rafeaie H, Mohd Yusop NF, Azmi NF, Abdullah NS, Ramli NIT. Photocatalytic degradation of methylene blue dye solution using different amount of ZnO as a photocatalyst. Sci Lett [Internet]. 2021 Jan 3;15(1):1-12. Available from: [<URL>](#).
13. Pakalapati H, Show PL, Chang JH, Liu BL, Chang YK. Removal of dye waste by weak cation-exchange nanofiber membrane immobilized with waste egg white proteins. Int J Biol Macromol [Internet]. 2020 Dec;165:2494-507. Available from: [<URL>](#).
14. Jawad AH, Abd Rashid R, Ismail K, Sabar S. High surface area mesoporous activated carbon developed from coconut leaf by chemical activation with H<sub>3</sub>PO<sub>4</sub> for adsorption of methylene blue. Desalin Water Treat [Internet]. 2017;74:326-35. Available from: [<URL>](#).
15. Abdulhameed AS, Mohammad AT, Jawad AH. Application of response surface methodology for enhanced synthesis of chitosan tripolyphosphate/TiO<sub>2</sub> nanocomposite and adsorption of reactive orange 16 dye. J Clean Prod [Internet]. 2019 Sep;232:43-56. Available from: [<URL>](#).
16. Tüzün E, Karakuş S. Ultrasound-Assisted Adsorption of Basic Blue 41 onto Salda mud: Optimization and Error Analysis. J Turkish Chem Soc Sect A Chem [Internet]. 2021 Feb 28;8(1):57-68. Available from: [<URL>](#).
17. Karaca H, Altıntiğ E, Türker D, Teker M. An evaluation of coal fly ash as an adsorbent for the removal of methylene blue from aqueous solutions: kinetic and thermodynamic studies. J Dispers Sci Technol [Internet]. 2018 Dec 2;39(12):1800-7. Available from: [<URL>](#).
18. Li H, Dai M, Dai S, Dong X, Li F. Methylene blue adsorption properties of mechanochemistry modified coal fly ash. Hum Ecol Risk Assess An Int J [Internet]. 2018 Nov 17;24(8):2133-41. Available from: [<URL>](#).
19. Zhou J, Xia K, Liu X, Fang L, Du H, Zhang X. Utilization of cationic polymer-modified fly ash for dye wastewater treatment. Clean Technol Environ Policy [Internet]. 2021 May 14;23(4):1273-82. Available from: [<URL>](#).
20. Burduhos Nergis DD, Abdullah MMAB, Sandu AV, Vizureanu P. XRD and TG-DTA Study of New Alkali Activated Materials Based on Fly Ash with Sand and Glass Powder. Materials (Basel) [Internet]. 2020 Jan 11;13(2):343. Available from: [<URL>](#).
21. Abdulhameed AS, Jawad AH, Mohammad AT. Synthesis of chitosan-ethylene glycol diglycidyl ether/TiO<sub>2</sub> nanoparticles for adsorption of reactive orange 16 dye using a response surface methodology approach. Bioresour Technol [Internet]. 2019 Dec;293:122071. Available from: [<URL>](#).
22. Surip SN, Abdulhameed AS, Garba ZN, Syed-Hassan SSA, Ismail K, Jawad AH. H<sub>2</sub>SO<sub>4</sub>-treated Malaysian low rank coal for methylene blue dye decolorization and cod reduction: Optimization of adsorption and mechanism study. Surfaces and Interfaces [Internet]. 2020 Dec;21:100641. Available from: [<URL>](#).
23. Hassan R, Arida H, Montasser M, Abdel Latif N. Synthesis of New Schiff Base from Natural Products for Remediation of Water Pollution with Heavy Metals in Industrial Areas. J Chem [Internet]. 2013;2013:240568. Available from: [<URL>](#).
24. Choudhary M, Kumar R, Neogi S. Activated biochar derived from Opuntia ficus-indica for the efficient adsorption of malachite green dye, Cu<sup>+2</sup> and Ni<sup>+2</sup> from water. J Hazard Mater [Internet]. 2020 Jun;392:122441. Available from: [<URL>](#).
25. Al-Ghouti MA, Da'ana DA. Guidelines for the use and interpretation of adsorption isotherm models: A review. J Hazard Mater [Internet]. 2020 Jul;393:122383. Available from: [<URL>](#).
26. Wang J, Guo X. Adsorption kinetic models: Physical meanings, applications, and solving methods. J Hazard Mater [Internet]. 2020 May;390:122156. Available from: [<URL>](#).
27. Hsu T. Adsorption of an acid dye onto coal fly ash. Fuel [Internet]. 2008 Oct;87(13-14):3040-5. Available from: [<URL>](#).
28. Ramakrishna KR, Viraraghavan T. Dye removal using low cost adsorbents. Water Sci Technol [Internet]. 1997;36(2-3):189-96. Available from: [<URL>](#).
29. Sun D, Zhang X, Wu Y, Liu X. Adsorption of anionic dyes from aqueous solution on fly ash. J Hazard Mater [Internet]. 2010 Sep;181(1-3):335-42. Available from: [<URL>](#).
30. Eren Z, Acar FN. Adsorption of Reactive Black 5 from an aqueous solution: equilibrium and kinetic studies. Desalination [Internet]. 2006 Jun;194(1-3):1-10. Available from: [<URL>](#).
31. Dizge N, Aydinler C, Demirbas E, Kobya M, Kara S. Adsorption of reactive dyes from aqueous solutions by fly ash: Kinetic and equilibrium studies. J Hazard Mater [Internet]. 2008 Feb;150(3):737-46. Available from: [<URL>](#).

